

# Two-Step Synthesis and Characterization of a New Disordered Mesoporous Manganese Silicate MnKIL-1

Alenka Ristić,\* Nataša Novak Tušar, Saša Cecowski, Matjaž Mazaj  
and Venčeslav Kaučič

National Institute of Chemistry, Hajdrihova 19, SI-1001 Ljubljana, Slovenia

\* Corresponding author: E-mail: alenka.ristic@ki.si

Received: 06-11-2008

## Abstract

New manganese silicate denoted as MnKIL-1 was prepared by two-step synthesis. Solvothermal treatment in ethanol in the second step of the synthesis gave rise of a disordered mesoporous silicate structure with the pore openings of 16 nm. The mesoporous property (porosity) of the new material was investigated by employing powder X-ray diffraction (XRD), transmission electron microscopy (TEM) and nitrogen sorption. UV-Vis diffuse reflectance spectroscopy results suggested that the  $\text{Mn}^{2+}$  and  $\text{Mn}^{3+}$  cations were coordinated in the mesoporous silicate structure in the disordered octahedral and tetrahedral environments, respectively.

**Keywords:** Mesoporous manganese silicate, MnKIL-1, nanomaterials, solvothermal treatment, porosity, UV-Vis spectroscopy

## 1. Introduction

The development of nanoporous inorganic materials is of great commercial and scientific interest. This interest has been driven by the potential for novel optical, electronic and magnetic properties<sup>1–3</sup> as well as the possibility of applications in areas such as energy storage, optical communications and drug delivery.<sup>4–7</sup> In each of these application areas, porous materials often serve different goals depending on their engineered design and synthesis. A large diversity in materials and their properties has been developed over the years, studied and evaluated by an interdisciplinary community ranging from chemist and physicists to medical doctors and mathematicians.

Manganese is an environmentally friendly active component for numerous catalyst systems.<sup>8</sup> To expand the available pore size range of highly ordered manganese containing porous silicates such as MnMCM-41 with pore widths of 4 nm<sup>9</sup> and MnSBA-15 with pore openings of 6 nm,<sup>10</sup> manganese containing foam-like MnTUD-1<sup>8</sup> with pore openings of 4–9 nm was recently prepared. TUD-1<sup>11</sup> and some other foam-like mesoporous silicates, including HMS,<sup>12</sup> MSU<sup>13</sup> and KIT-1<sup>14</sup> show disordered mesopores

and amorphous pore walls. 3D pores in disordered mesostructures are interpenetrating, uniform and adjustable. The characteristics of disordered mesostructures, such as uniform pores, high surface areas and easy modification offer good opportunities in catalysis, adsorption, separation and immobilization.<sup>15</sup>

In this manuscript, we present a two-step synthesis and characterization of new disordered mesoporous manganese silicate MnKIL-1 (KIL denotes Kemijski Inštitut Ljubljana) with pore openings of 16 nm. The synthesis procedure is cost-effective and environmental friendly, because it is surfactant-free. A non-surfactant synthesis of mesoporous materials still represents a great challenge because few molecules with size of several nanometers possess suitable spatial structure to direct the further construction.

## 2. Experimental

### 2. 1. Synthesis

MnKIL-1 was prepared by a two-step method according to the modified templating method of Jansen et al<sup>11</sup>. In the synthesis procedures, 0.57 g of manganese acetate

trahydrate ( $\text{Mn}(\text{CH}_3\text{COO})_2 \cdot 4\text{H}_2\text{O}$ , Aldrich) was added to 24.75 g of tetraethyl orthosilicate (99% TEOS, Alfa Aesar) while stirring. 9.05 g of triethanol amine (97% TEA, Fluka), 19.55 g of deionized water and 4.95 g of tetraethylammonium hydroxide (35% TEOH, Fluka) were added dropwise to the previous solution, respectively. The solutions were mixed with magnetic stirrer to obtain homogeneous solid gel with a molar ratio composition of 1 TEOS : 0,5 TEA : 0,02  $\text{MnO}$  : 0,1 TEOH : 11  $\text{H}_2\text{O}$ . The mixture was aged at room temperature for 24 hours and then dried at 100 °C over night (a first step). In the second step, the clear solid gel was solvothermally treated in ethanol at 150 °C for 2 days using 30  $\text{cm}^3$  Teflon-lined stainless steel autoclave. The obtained solid product was washed with ethanol and dried in an oven at 50 °C. Surfactant-free MnKIL-1 was prepared by the removal of the triethanol amine and the tetraethylammonium hydroxide by calcination at 500 °C for 10 h using a ramp rate of 1 °C/min in the flow of air.

## 2. 2. Characterization

XRD patterns were obtained on a Siemens D5000 using  $\text{CuK}\alpha$  radiation ( $\lambda = 1,5406 \text{ \AA}$ ). The sample was scanned over a range of 0.5–10°  $2\theta$  with a step of 0.04° and in the range of 5 to 60°  $2\theta$  with the step of 0.02° to detect the mesostructure and the presence of manganese oxides, respectively.

The mesostructure was also investigated by TEM on a 200-kV field-emission gun (FEG) microscope JEOL JEM 2010F. For TEM studies the sample was dispersed in ethanol and placed on a copper holey carbon grid.

SEM micrograph was obtained by scanning electron microscopy on Zeiss Supra<sup>TM</sup> 3VP microscope.

Elemental analysis was performed by EDX method with INCA Energy system attached to Zeiss Supra<sup>TM</sup> 3VP microscope.

Nitrogen physisorption measurement was performed on a Micromeritics ASAP 2020 volumetric adsorption analyzer. Before the adsorption analysis, the sample was out gassed under vacuum for 2 h at 473 K in the port of the adsorption analyzer. The BET specific surface area,  $^{16}S_{\text{BET}}$ , was calculated using the adsorption branch in the relative pressure range between 0.05 and 0.25. The total pore volume was estimated from the amount adsorbed at a relative pressure of 0.98, converting it to the volume of liquid nitrogen at 77 K. The mesopore volume,  $V_p$ , the external surface area,  $S_{\text{ex}}$ , and the total surface area,  $S_t$ , were determined using the  $\alpha_s$ -plot method<sup>17</sup> from the adsorption data for mesostructured MnKIL-1. The same method was applied to show the lack of microporosity<sup>18</sup> in this material. LiChrospher Si-1000 silica gel was used as a reference solid in the  $\alpha_s$ -plot analysis.<sup>19</sup> The mesopore size distribution (PSD) was calculated from nitrogen adsorption data using Barrett, Joyner, and Halenda (BJH) method.<sup>20</sup> The maximum on the PSD was considered as the primary mesopore diameter for given sample.

Diffuse reflectance UV-Vis spectra of the sample as well as of reference material were recorded at room temperature using a Perkin-Elmer Lambda 40P UV-VIS spectrophotometer equipped with the RSA-PE-19M Praying Mantis accessory, which is designed for diffuse reflectance measurements of horizontally positioned powder samples, pastes or rough surface samples. The Spectralon<sup>®</sup> white reflectance standard was used to perform the instrument background correction in the range of 200–800 nm.

## 3. Results and Discussion

The low-angle powder XRD pattern shown on Figure 1A exhibited a single broad diffraction peak in the range between 0.7 and 2°  $2\theta$  with a maximum at 0.97°  $2\theta$ . This diffraction peak was not observed when the second step of the synthesis (solvothermal treatment) was not performed. Single broad diffraction peak indicated disordered mesoporous MnKIL-1 with wide pore size distribution. High-angle XRD was employed to detect the presence of manganese oxides in mesoporous MnKIL-1. High-angle powder XRD pattern (Fig. 1B) showed only two diffraction peaks at 38.29°  $2\theta$  and 44.46°  $2\theta$  corresponding to aluminium sample holder. XRD pattern did not show any diffraction peaks corresponding to manganese oxide phases as it was indicated from the results of  $\text{N}_2$  sorption analysis and diffuse reflectance UV-Vis spectroscopy, described below. This could be explained with the presence of highly dispersed manganese oxide clusters with nanosized dimensions that were not detectable by XRD technique and were located on the surface and within the mesopores.

Mesostructure of MnKIL-1 was investigated by transmission electron microscopy (TEM) and nitrogen sorption. Figure 2A showed typical TEM image with disordered porous structure. TEM image revealed that this disordered mesoporous material possessed pore openings

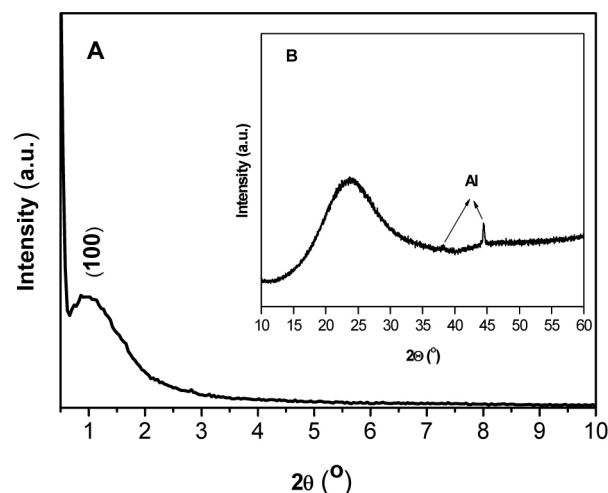


**Figure 1:** Low-angle XRD (A) and high-angle XRD (B Inset) patterns of new mesoporous MnKIL-1.

in very broad range of dimensions (5–20 nm) which corresponded to low-angle XRD measurements. Mesoporous MnKIL-1 was shown by SEM micrograph (Figure 2B).

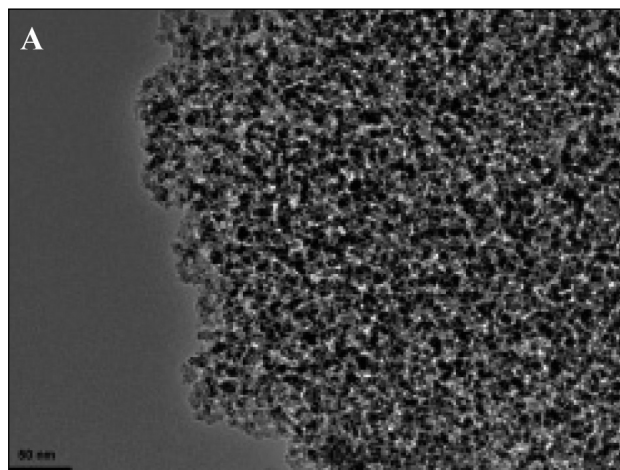


**Figure 2:** TEM image (A) and SEM micrograph (B) of new mesoporous MnKIL-1.

Nitrogen sorption isotherm for mesoporous MnKIL-1 was shown in Figure 3, whereas structural parameters determined on the basis of this isotherm were listed in Table 1. The nitrogen adsorption-desorption isotherm for the sample studied was typical type-IV isotherm<sup>21,22</sup> with a steep increase of adsorption branch at  $p/p_0$  0.75–0.95 due to the capillary condensation of nitrogen in the mesopores. The BET surface area of the sample was  $591 \text{ m}^2 \text{ g}^{-1}$ . No micropores were present in MnKIL-1 according to  $\alpha_s$ -plot method.

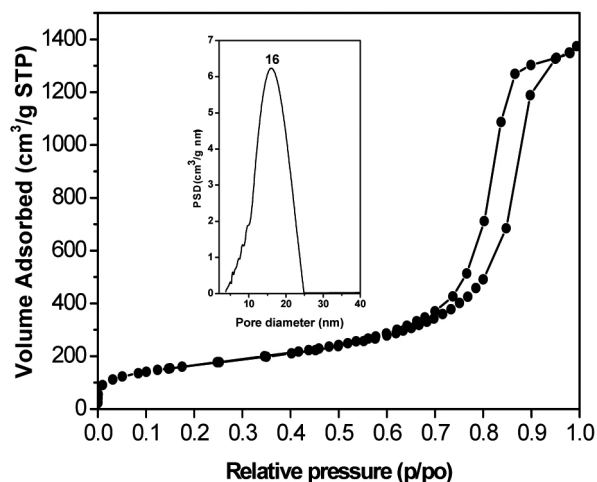


**Figure 3:** Nitrogen sorption isotherm with pore size distribution curve (Inset) of new mesoporous MnKIL-1.

The pore size distribution (PSD) obtained from the adsorption isotherm by BJH method was rather broad having a maximum at the pore width of 16 nm. The pore size distribution curve indicated smaller pore size uniformity as it was revealed from the results of low-angle XRD measurements and TEM micrograph, i.e. this disordered mesoporous material possessed pore widths from 5 to 25 nm.

The presence of the manganese, placed in the framework, and manganese oxides, located in pores and on the surface of the mesoporous MnKIL-1, was characterised by diffuse reflectance UV–Visible spectroscopy. Two broad bands at 270 and 480 nm were observed for this sample in Figure 4. A band at 270 nm have been ascribed to the charge transfer transition of  $\text{O}^{2-} \rightarrow \text{Mn}^{3+}$  in tetrahedral coordination, indicating the incorporation of manganese in the framework of MCM-41.<sup>23</sup> The broad band at 480 nm was assigned to octahedral coordination of  $\text{Mn}^{2+}$  in  $\text{Mn}_2\text{O}_3$  or  $\text{MnO}$ , probably existing on the surface of mesoporous manganese silicate.<sup>24</sup>

The presence of manganese oxides in pores were found also by the nitrogen adsorption-desorption isotherm (Figure 3) with a small tailing of hysteresis loop, indicating on the presence of manganese oxides plugs.<sup>25</sup>

The high surface area, large pore openings and manganese, placed in the framework, with manganese oxides, located in pores and on the surface make this new material MnKIL-1 excellent candidate for catalysis and energy storage.

**Table 1:** Textural properties of mesoporous MnKIL-1

Sample	Si/Mn (m <sup>2</sup> /g)	$S_{\text{BET}}$ (cm <sup>3</sup> /g)	$V_t$ (cm <sup>3</sup> /g)	$V_{\text{me}}$ (m <sup>2</sup> /g)	$S_{\text{ex}}$ (m <sup>2</sup> /g)	$S_t$ (nm)	$w_{\text{BJH}}$
MnKIL-1	21.5	519	2.08	1.92	90	497	16.0

Abbreviations:  $S_{\text{BET}}$ , the BET surface area;  $V_t$ , total pore volume evaluated from adsorption isotherm at the relative pressure about 0.994;  $V_{\text{me}}$ , primary mesopore volume;  $S_{\text{ex}}$ , external surface area;  $S_t$ , total surface area;  $w_{\text{BJH}}$ , mesopore diameter.

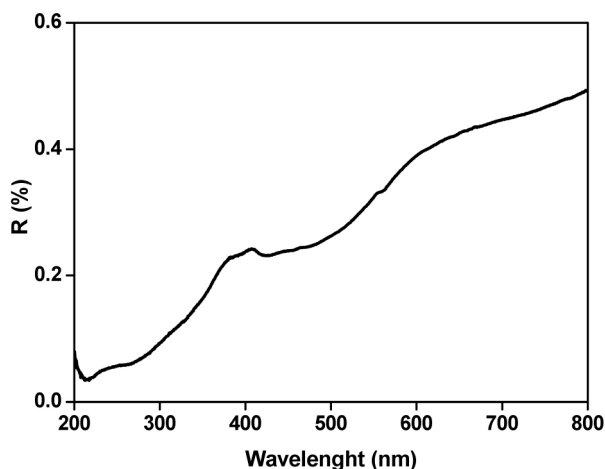


Figure 4: DR UV-Vis spectrum of new mesoporous MnKIL-1.

## 4. Conclusion

In summary, new mesoporous manganese silicate named MnKIL-1 can be synthesised using a cost-effective and environmental friendly two-step preparation method. MnKIL-1 has a disordered porous structure with a rather broad pore size distribution centred at 16 nm and high surface area of  $591 \text{ m}^2 \text{ g}^{-1}$ . The part of manganese cations in the  $\text{Mn}^{3+}$  form is probably incorporated in the silicate porous framework, while manganese cations  $\text{Mn}^{2+}$  are present in the form of manganese oxides located in the pores and on the surface of the material.

## 5. Acknowledgement

We thank for the support by the Slovenian Research Agency through the research program P1-0021-0104.

## 6. References

1. R. F. Ziolo, E. P. Giannelis, A. B. Weinstein, M. P. O'Horo, B. N. Ganguly, V. Mehrotra, W. Russell, D. R. Huffman, *Science*, **1992**, 257, 219–223.
2. Z. R. Tian, W. Tong, J. Y. Wang, N. G. Duan, V. V. Krishnan, S. L. Suib, *Science*, **1997**, 276, 926–930.
3. D. L. Leslie-Pelecky, R. D. Rieke, *Chem. Mater.*, **1996**, 8, 1770–1783.
4. L. F. Nazar, G. Goward, F. Leroux, M. Duncan, H. Huang, T. Kerr, J. Gaubicher, *Int. J. Inorg. Mater.*, **2001**, 3, 191–200.
5. N. Bai, S. G. Li, H. Y. Chen, W. Q. Pang, *Mater. Chem.*, **2001**, 11, 3099–3102.
6. N. Tessler, V. Medvedev, M. Kazes, S. Kan, U. Banin, *Science*, **2002**, 295, 1506–1508.
7. T. Heikkilä, J. Salonen, J. Tuura, M. S. Hamdy, G. Mul, N. Kumar, T. Salmi, D. Yu. Murzin, L. Laitinen, A. M. Kaukonen, J. Hirvonen, V.-P. Lehto, *Int. J. Pharm.*, **2007**, 331, 133–138.
8. A. Ramanathan, T. Archipov, R. Maheswari, U. Hanefeld, E. Roduner, R. Gläser, *J. Phys. Chem. C*, **2008**, 112, 7468–7476.
9. S. Vetrivel, A. Pandurangam, *Catal. Lett.*, **2008**, 120, 71–81.
10. M. Selvaraj, T. G. Lee, *J. Phys. Chem. B*, **2006**, 110, 21793–21802.
11. J. C. Jansen, Z. Shan, L. Marchese, W. Zhou, N. van der Puil, Th. Maschmeyer, *Chem. Commun.*, **2001**, 713–714.
12. P. T. Tanev, T. J. Pinnavaia, *Science*, **1995**, 267, 865–867.
13. S. A. Bagshaw, E. Prouzet, T. J. Pinnavaia, *Science*, **1995**, 269, 1242–1244.
14. R. Ryoo, J. M. Kim, C. H. Ko, C. H. Shin, *J. Phys. Chem.*, **1996**, 100, 17718–17721.
15. D. Zhao, Y. Wan, in: J. Čejka, H. Van Bekkum, A. Corma, F. Schuth (Ed.): *Introduction to Zeolite Science and Practice*, Elsevier, Amsterdam, **2007**, pp. 241–300.
16. S. Brunauer, P. H. Emmett, E. Teller, *J. Am. Chem. Soc.*, **1938**, 60, 309–319.
17. A. Sayari, P. Liu, M. Kruk, M. Jaroniec, *Chem. Mater.*, **1997**, 9, 2499–2506.
18. M. Kruk, M. Jaroniec, C. H. Ko, R. Ryoo, *Chem. Mater.*, **2000**, 12, 1961–1968.
19. B. Tan, H. J. Lehmler, S. M. Vyas, B. L. Knutson, S. E. Rankin, *Nanotechnology* **2005**, 16, 502–507.
20. E. P. Barrett, L. G. Joyner, P. P. Halenda, *J. Am. Chem. Soc.*, **1951**, 73, 373–380.
21. K. S. W. Sing, D. H. Everett, R. A. Haul, L. Moscou, R. A. Pirrotti, J. Rouquerol, T. Siemieniowska, *Pure Appl. Chem.*, **1985**, 57, 603–619.
22. S. S. Kim, T. R. Pauly, T. J. Pinnavaia, *Chem. Commun.*, **2000**, 1661–1662.
23. Q. Zhang, Y. Wang, S. Itsuki, T. Shishido, K. Takehira, *J. Mol. Catal. A*, **2002**, 188, 189–200.
24. M. Selvaraj, P. K. Sinha, K. Lee, I. Ahn, A. Pandurangan, T. G. Lee, *Micropor. Mesopor. Mater.*, **2005**, 78, 139–149.
25. E. B. Celer, M. Kruk, Y. Zuzek, M. Jaroniec, *J. Mater. Chem.*, **2006**, 16, 2824–2833.

## Povzetek

Nov mezoporozni manganov silikat imenovan MnKIL-1 smo pripravili z dvostopenjsko sintezo. Solvothermalna obdelava v etanolu v drugi sintezni stopnji je povzročila nastanek neurejene mezoporozne silikatne strukture s porami velikosti 16 nm. Poroznost novega materiala smo preiskovali z uporabo praškovne rentgenske difrakcije (XRD), presežno elektronsko mikroskopijo (TEM) in dušikovo sorpcijo. Rezultati difuzijske refleksijske UV-Vis spektroskopije kažejo, da so  $\text{Mn}^{2+}$  kationi oktaedrično,  $\text{Mn}^{3+}$  kationi pa tetraedrično koordinirani v mezoporozni silikatni strukturi.